Available online at www.sciencedirect.com
SCIENCE DIRECT®
Carbohydrate Research 339 (2004) 2549–2554
Carbohydrate RESEARCH

Metal-ion environment in solid Mn(II), Co(II) and Ni(II) hyaluronates

Elizabeta Tratar Pirc,[a,*] Iztok Arčon,[b,c] Alojz Kodre[c,d] and Peter Bukovec[a]

[a]*Faculty of Chemistry and Chemical Technology, Aškerčeva 5, SI-1000 Ljubljana, Slovenia*
[b]*Nova Gorica Polytechnic, Vipavska 13, SI-5000 Nova Gorica, Slovenia*
[c]*Jozef Stefan Institute, Jamova 39, SI-1000 Ljubljana, Slovenia*
[d]*Faculty of Mathematics and Physics, University of Ljubljana, Slovenia*

Received 7 May 2004; accepted 22 July 2004
Available online 18 September 2004

Abstract—Amorphous powders and films of some metal hyaluronate complexes of general composition $(C_{14}H_{20}O_{11}N)_2 \cdot xH_2O$ (M = Mn^{2+}, Ni^{2+} and Co^{2+}) have been prepared at pH 5.5–6.0. The coordination geometry around the metal ions has been analyzed by EXAFS (extended X-ray absorption fine structure) and FTIR spectroscopy. Mn^{2+}, Ni^{2+}, and Co^{2+} ions are coordinated to carboxylate oxygen atoms and water molecules. The process of local geometry formation round the metal ions is sensitive to sample preparation.

Keywords: Metal hyaluronate; EXAFS; FTIR; Conformation

1. Introduction

The glycosaminoglycan, hyaluronan (hyaluronic acid, HA), is becoming increasingly important as many biological functions and biomedical applications for it are discovered.[1–3] HA is the most abundant in animal connective tissues. In these substrates HA occurs in the stable salt form as sodium hyaluronate, usually associated with proteins.[4] HA can be found in the skin, vitreous humour, cartilage and umbilicard cord. It controls the hydration level of tissues, maintains interstitial fluid volume, organizes the extracellular matrix, and has an immunosuppressive function.[5] Recent work has demonstrated that HA also greatly influences diverse biological processes such as cell adhesion, proliferation, migration and differentiation.[6]

HA is a heteropolysaccharide composed of the disaccharide unit (-GlcNAc-β-(1 → 4)-GlcA-β-(1 → 3)-)$_n$ where GlcA is D-glucuronic acid and GlcNAc is 2-acetamido-2-deoxy-D-glucose (*N*-acetyl-D-glucosamine) and *n* is approximately 10^4 (Fig. 1).

Under physiological conditions, HA is a negatively charged polyelectrolyte due to repeating anionic carboxylic sites.[7] Each disaccharide unit requires a positive metal ion for the charge neutrality. The interaction of the polyanion with the cations is an important factor for the supermolecular structure.[8] The coordination geometry of the ion exerts a strong influence on the conformation of the macromolecule and its biological activity.

Most macromolecular ligands are biologically active compounds that play important roles in life processes (e.g., proteins, carbohydrates, nucleic acids, etc.), behaviour, which cannot be expected for their small molecular

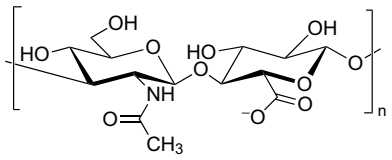

Figure 1. Structure of hyaluronate (HA) chain.

* Corresponding author. Fax: +386 241 9220; e-mail: elizabeta.tratar@uni-lj.si

0008-6215/$ - see front matter © 2004 Elsevier Ltd. All rights reserved.
doi:10.1016/j.carres.2004.07.025

fragments. Metal complexation may change their biologically activity, and the new properties may be utilized in many cases in pharmaceutical practice.[9] The salts of HA formed with alkaline, alkaline earth, aluminium or ammonium ions may serve as carriers for promoting the absorption of drugs.[10,12] Sodium salts are used in therapy, mainly in opthalmology, surgery and cosmetics.[10,11]

Very few references relating to complexes of HA formed with 3d metal ions of the fourth period of the periodic table can be found in the literature. HA has been shown to coordinate to Cu^{2+}, Ag^{1+}, Au^{3+}, Cd^{2+}, Pb^{2+}, Fe^{3+} and Zn^{2+} in solutions.[13–16] Hyaluronate complexes with heavy metals show microbicidal activity. Gold complexes are used in arthritis therapy; platinum complexes have antitumour activity.[17]

Solid metal hyaluronates have not been extensively studied. Amorphous copper(II) hyaluronate of composition $(Cu(C_{14}H_{20}O_{11}N)_2{\cdot}6H_2O)_n$ was prepared at pH 5.5 by precipitation from water solutions with cold ethanol. The local structure around copper ion was determined by EXAFS and XANES method.[18] The coordination geometry around copper ion is a disordered octahedron. The four equatorial sites are occupied by oxygen atoms at an average distance of 195 pm. For the two axial sites at a larger distance of 246 pm, oxygen atoms are preferentially indicated.

A zinc(II) hyaluronate (ZnHA) complex is formed by addition of Zn(II) chloride to an aqueous solution of sodium hyaluronate at a pH value between 5.5 and 6.5. The complex, which can be precipitated from the solution by ethanol or methanol, has been patented and used for ulcer treatment.[19] The EXAFS and XANES methods showed that Zn^{2+} ion is coordinated to four oxygen atoms with a Zn–O bond distance of 202 pm. Two carbon atoms at distance 299 pm were detected in the second coordination sphere.[20]

There is no literature data about manganese(II), nickel(II) and cobalt(II) hyaluronates. These complexes or their derivates could be potentially new biomaterials, which could facilitate the formation of polymeric films (or gels) and could be used in different fields (medicine, pharmacy, etc.).

The present study is focused on the interaction of the HA molecule with manganese(II), nickel(II) and cobalt- (II) ions, in particular on the differences in ion coordination that influences the behaviour of the whole macromolecule. The coordination geometry around Mn^{2+}, Ni^{2+} and Co^{2+} ions is analyzed by EXAFS and FTIR. The relaxation process of the complexation is probed by preparation of two forms of the solid product. A powder form is obtained in a fast precipitation of the metal hyaluronates from water solutions with ethanol. Slow drying of metal hyaluronate water solutions, whereby the conformation of the macromolecule is fully relaxed, results in pliable films.

2. Materials and methods

2.1. Preparation of powdered metal hyaluronates and metal hyaluronate films

Sodium hyaluronate (NaHA) samples of highest purity were obtained from ARD (France), with molecular weight approximately 2×10^5 D and a water content of 7.5% as determined by thermogravimetry. Analytical grade $MnCl_2{\cdot}4H_2O$, $NiCl_2{\cdot}6H_2O$ and $CoCl_2{\cdot}6H_2O$ were used without further purification.

For preparation of a powdered metal hyaluronate, 0.50 g of NaHA was weighed into a 50-mL volumetric flask and after addition of 30 mL of distilled water, left to swell for several hours. A solution (11.5 mL) of 0.10 M MCl_2 ($M = Mn^{2+}$, Ni^{2+} or Co^{2+}) was added, and the resulting mixture was stirred for 1 h. The pH of the solution (Mettler Toledo 220) was adjusted with 0.01 M HCl to pH 5.5–6.0. Cold absolute ethanol was added under vigorous stirring. A green, pink or white precipitate appeared in respective cases of Ni^{2+}, Co^{2+} and Mn^{2+} addition. The adjustment of pH was vital since at pH values above 6.0 a viscous solution was formed and a homogeneous powdered product could not be precipitated. The products were filtered using a glass filter, washed twice with 25 mL of ethanol and dried in a desiccator over silica gel. Elemental analysis for C, H, N was conducted on a Perkin–Elmer 2400 CHN Microanalyser. The metals were determined by complexometry and thermogravimetry. The results per disaccharide unit are given in Table 1.

For the preparation of a metal hyaluronate film, 0.50 g of NaHA was weighed into a 50-mL beaker, 15 mL of distilled water was added, and the mixture was left to swell for several hours. MCl_2 solution

Table 1. Elemental analysis of synthesized metal hyaluronates

Element	Exp. (%)	Theor. (%)
$Co(C_{14}H_{20}O_{11}N)_2{\cdot}6H_2O$ (CoHA)		
C	36.28	36.41
H	5.97	5.64
N	2.99	3.03
Co TG	6.24	6.38
Compl	6.2	
$Ni(C_{14}H_{20}O_{11}N)_2{\cdot}7H_2O$ (NiHA)		
C	35.91	35.72
H	6.03	5.78
N	2.98	2.98
Ni TG	6.240	6.38
Compl	6.0	
$Mn(C_{14}H_{20}O_{11}N)_2{\cdot}8H_2O$ (MnHA)		
C	34.95	35.19
H	6.12	5.91
N	2.91	2.93
Co TG	6.24	5.75
Compl	6.2	

(5.3 mL, 0.1 M) was added, and the solutions were mixed well at 600 rpm. The pH values of the resulting solution was adjusted with 0.01 M HCl to pH 5.5–6.0. The viscous solution was dried slowly at a temperature not exceeding 35 °C to obtain a homogeneous film.

2.2. FTIR spectroscopy

FTIR spectra of isolated powdered metal hyaluronates CoHA, NiHA and MnHA and of the starting material NaHA were recorded in the range from 4000 to 600 cm^{-1}. A Digilab division FTIR spectrophotometer with KBr windows was used. FTIR spectra of the films could not be obtained because the reflection was too high.

2.3. EXAFS

The Mn, Co and Ni K-edge EXAFS spectra of hyaluronate powders and films were measured at the E4 beamline of HASYLAB synchrotron radiation facility at DESY, Hamburg. The station provides a focused beam from an Au-coated mirror and a Si(1 1 1) double-crystal monochromator with ~1 eV resolution at the Co K-edge. Harmonics were effectively eliminated by a plane Au-coated mirror and by detuning the monochromator crystals to 60% of the rocking curve with the beam stabilization feedback control. Powdered metal hyaluronate samples were prepared on multiple layers of adhesive tape, while films required no support. The thickness of each sample was chosen to obtain optimal absorption of ~1 above the investigated absorption edge. Reference spectra were measured on empty tapes. The exact energy calibration was established with the simultaneous absorption scan on the respective metal sample (Co and Ni metal foil, Mn metal powder).

3. Results

3.1. FTIR spectroscopy

FTIR spectra of CoHA, NiHA and MnHA powder samples and of the starting material NaHA are compared in Figure 2. The polymer molecule has carboxyl and acetamido characteristic groups, and numerous hydroxyl groups on glycopyranoside rings that give rise to complex absorption features in the spectra. Individual absorption bands in the spectrum of the NaHA compound were assigned by Gilli et al.[21]. The spectra of all three powdered metal hyaluronates are very similar to that of NaHA, so basically the same assignations can be adopted. In the following we therefore comment only on the characteristic and significant differences.

The spectra reveal that after a replacement of sodium ion in NaHA with Co^{2+}, Ni^{2+} or Mn^{2+} ion, only the

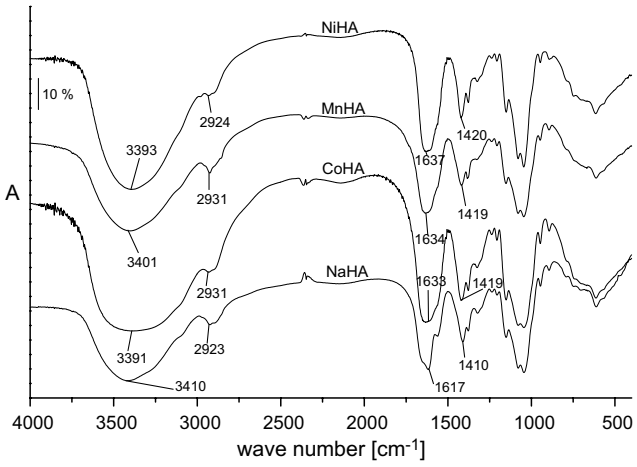

Figure 2. FTIR spectra of CoHA, NiHA and MnHA powder samples and corresponding starting material NaHA.

carboxyl absorption bands are shifted significantly, indicating the bonding of the metal ion to the carboxylate group. According to Deacon and Phillips[22] a carboxylate ion can coordinate to metals in a number of ways: as a unidentate, chelating or bridging ligand or in an arrangement involving combined chelation and bridging.

In unidentate coordination the equivalence of the two oxygen atoms in the carboxylate ion is removed, whereby the separation between symmetric and asymmetric vibrational frequencies is increased. The characteristic frequencies $\nu(C–O)_{sym}$ and $\nu(C–O)_{asym}$, respectively, for the symmetric and asymmetric vibrational modes in solid CoHA, NiHA, MnHA and in the reference NaHA are shown in Table 2. The separation of 216 cm^{-1} of the two vibrational frequencies (Δ) in isolated complexes is slightly larger than in NaHA (207 cm^{-1}), indicating that the carboxylate group is unidentately bound to the metal ion.

3.2. EXAFS

EXAFS spectra were analyzed with the University of Washington UWXAFS package[23] using the FEFF6 code for ab initio calculation of scattering paths.[24] Fourier transforms of k^3 weighted Mn, Co and Ni EXAFS spectra calculated in the k-range 4–12 $Å^{-1}$ are shown

Table 2. The characteristic frequencies for the symmetric and asymmetric vibrational modes in solid CoHA, NiHA, MnHA and NaHA

Metal ion	ν_{asym} (cm^{-1})	ν_{sym} (cm^{-1})	Δ (cm^{-1})
Mn^{2+}	1635	1419	216
Co^{2+}	1634	1419	215
Ni^{2+}	1637	1420	217
Na^{+}	1617	1410	207

Separation (Δ) of the vibrational frequencies is also given.

in Figures 3–5, respectively, together with the best-fit EXAFS models. Fit parameters are listed in the Table 3.

In the model of Co EXAFS spectrum (Fig. 3), the best fit of the first coordination shell in the R range 1.3–2.3 Å shows that in the powder sample as well as in the film, the cobalt atoms are coordinated to four oxygen atoms at 2.06 Å. The presence of an additional shell composed of two loosely bound oxygen atoms at a much larger distance of 2.39 Å is found in the film. A large value of the Debye–Waller factor obtained for this shell is an indication of a large spread of the bond distance, caused either by a static disorder or by a stronger effect of the thermal motion due to a weak bond.

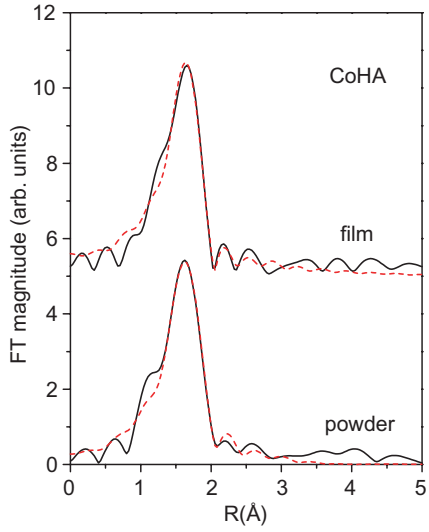

Figure 3. Fourier transforms of k^3 weighted EXAFS spectra of Co(II) hyaluronate powder and film sample (experiment, — solid line, EXAFS model, --- dashed line).

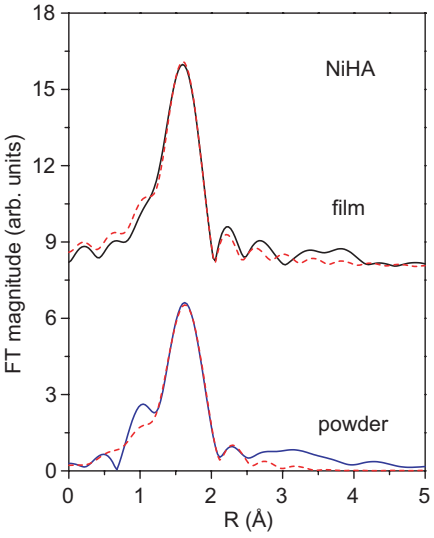

Figure 4. Fourier transforms of k^3 weighted EXAFS spectra of Ni(II) hyaluronate powder and film sample (experiment, — solid line; EXAFS model, --- dashed line).

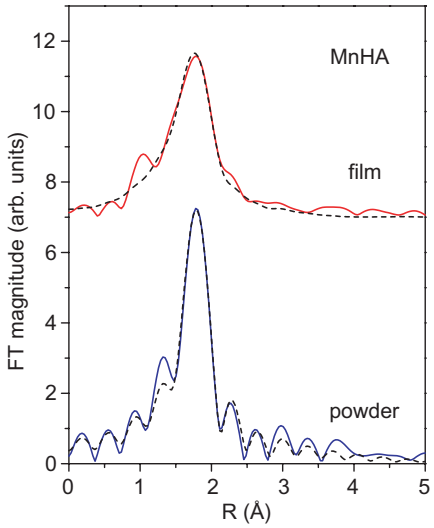

Figure 5. Fourier transforms of k^3 weighted EXAFS spectra of Mn(II) hyaluronate powder and film sample (experiment, — solid line, EXAFS model, --- dashed line).

The model of the Ni EXAFS spectrum (Fig. 4), in the R range 1.3–2.2 Å shows that nickel atoms are coordinated to six oxygen atoms at 2.06 Å in the powdered sample and in the film. The relatively large Debye–Waller factors indicate a possible distortion of the oxygen octahedron.

The best fit of the model of the Mn EXAFS spectrum (Fig. 5), in the R range 1.3–2.4 Å shows that manganese(II) is coordinated to six oxygen atoms in both samples. A distorted octahedron coordination is indicated by the model: the best fit is found with four oxygen neighbours at about 2.15 Å and two at about 2.3 Å. A larger disorder in the first coordination shell is observed in the film.

4. Discussion

FTIR and EXAFS analyses reveal the coordination geometry around metal ions in the hyaluronate complexes. Mn^{2+}, Ni^{2+}, and Co^{2+} ions are unidentately coordinated to carboxylate oxygen atoms and to water molecules. Figure 6 shows the proposed structure of the complexes.

EXAFS spectra of the NiHA and MnHA complex showed that Ni^{2+} and Mn^{2+} ions are octahedrally coordinated in both forms: in powder and in film. The coordination of these two ions is therefore not sensitive to the sample preparation. The octahedron around Ni(II) is regular, while the Mn(II) neighbourhood exhibits distortion. However, the Mn–O distances are significantly larger than in other 6-coordinated Mn^{2+} complexes,[25]

Table 3. Parameters of the nearest coordination shell of oxygen atoms around metal atoms in hyaluronates

Metal ion	Powder			Film		
	N	*r* (Å)	σ^2 (Å^2)	*N*	*r* (Å)	σ^2 (Å^2)
Co^{2+}	4.0(1)	2.058(4)	0.0075(4)	4.2(7)	2.07(1)	0.007(1)
				2.0(7)	2.39(1)	0.033(1)
Ni^{2+}	6.0(5)	2.056(2)	0.0066(8)	6.4(4)	2.06(2)	0.0066(5)
Mn^{2+}	3.9(5)	2.17(2)	0.002(2)	4.0(2)	2.14(2)	0.007(2)
	1.4(7)	2.33(4)	0.002(2)	2.0(2)	2.26(4)	0.006(2)

N, average number; *R*, metal–oxygen distance; and σ^2, Debye–Waller factor. Uncertainty of the last digit is given in parentheses.

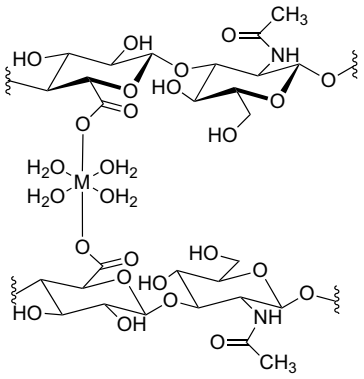

Figure 6. Proposed structure for metal hyaluronates. The coordination number for manganese(II) and nickel(II) hyaluronate is 6. In case of cobalt(II) hyaluronate 4 (two water molecules less).

but in the same range as reported for Mn–glucuronate.[26,27]

The coordination geometry around Co^{2+} ion in CoHA complexes is basically different. In CoHA powder and film we found that Co is directly coordinated to four oxygen atoms.

In the CoHA film the evidence of two additional loosely bound oxygen atoms at much larger distance, most probably originating from coordinated water molecules, is found in the EXAFS signal. A similar, but weaker coordination of two water molecules to Co atoms in the powdered CoHA sample is not completely excluded, but its contribution to the EXAFS signal was under the detection limit. The coordination of water molecules in the process of film formation is sensitive to the conditions of synthesis. Such weak coordination may become more expressed during the slow relaxation of the structure in case of film formation than in fast precipitation of powder.

5. Conclusions

The structural results of CoHA, NiHA and MnHA compounds give insight into the process of formation of local geometry round the metal ions and the conformation of the HA chain. Two mechanisms compete: an extensive H-bond network interaction between water molecules and the HA chain on one hand and the electrostatic interactions between metal cations and carboxylate groups on the other. In case of more electropositive cations (Co^{2+} and Ni^{2+}), the electrostatic interaction prevails and the conformation of the HA chain is dictated by the metal-ion bonded to the chain. The less electropositive Mn^{2+} cation, on the other hand, cannot induce the necessary structural changes of the HA chain to accommodate local coordination of oxygen atoms. The conformation of the HA chain is thus dictated by the stronger H-bond network interaction, and Mn^{2+} cations occupy the available electrostatic holes around the carboxylate groups.

This conclusion is also supported by the results of thermal stability of the metal hyaluronate complexes. NiHA and CoHA show a similar thermal stability, while MnHA decomposes at a lower temperature.[28]

Acknowledgements

The authors gratefully acknowledge the Ministry of Education, Science and Sport of the Republic of Slovenia for the financial support of the present study within the research program P1-0112, the European Commission support IHP-Contract HPRI-CT-1999-00040/2001-00140 and the bilateral project BI-DE/03-04-004 by Internationales Buero des BMBF. Access to synchrotron radiation facilities HASYLAB (project II-01-44) is acknowledged. K. Klementiev of HASYLAB provided expert advice on E4 beamline operation.

References

1. Barbucci, R.; Mangani, A.; Rappuoli, R.; Lamponi, S.; Consumi, M. *J. Inorg. Biochem.* **2000**, *79*, 125–199.
2. Cascone, M. G. *Polym. Int.* **1997**, *43*, 55–69.
3. Savani, R. C.; Cao, G.; Pooler, P. M.; Zaman, A.; Zhou, Z.; DeLisser, H. M. *J. Biol. Chem.* **2001**, *276*, 36770–36778.
4. Faser, J. R. E.; Laurent, T. C. In *Extracellular Matrix, Molecular Components and Interactions*; Comper, W. D.,

Ed.; Harwood Academic: Amsterdam; Vol. 2, pp 141–199.
5. Lee, J. Y.; Spicer, A. P. *Curr. Opin. Cell Biol.* **2000**, *12*, 581–586.
6. Zimmerman, E.; Geiger, B.; Addadi, L. *Biophys. J.* **2002**, *82*, 1848–1857.
7. Cleland, R. L.; Wang, J. L.; Detzweiler, D. M. *Macromolecules* **1982**, *15*, 386–395.
8. Moulabi, M.; Broch, H.; Robert, L.; Vasilescu, D. *J. Mol. Struct. (Theochem)* **1997**, *395–396*, 477–508.
9. Burger, K.; Illes, J.; Gyurcsik, B.; Gazdag, M.; Forrai, E.; Dekany, I.; Mihalyfi, K. *Carbohydr. Res.* **2001**, *332*, 197–207.
10. Gosh, P. *Clin. Exp. Rheumatol.* **1994**, *12*, 75–82.
11. Reiger, M. M. *Cosmet. Toiletries* **1998**, *113*, 35–48.
12. Goa, K. L.; Benfield, P. *Drugs* **1994**, *47*(3), 536–566.
13. Figueroa, N.; Nagy, B.; Chakrabarti, B. *Biochem. Biophys. Res. Commun.* **1977**, *74*, 460–465.
14. Sipos, P.; Veber, M.; Illes, J.; Machula, G. *Acta Chim. Hung.* **1992**, *129*(5), 671–683.
15. Sterk, H.; Braun, M.; Schmut, O.; Feichtinger, H. *Carbohydr. Res.* **1995**, *145*, 1–11.
16. Merce, A. L. R.; Carrera, L. C. M.; Romanholi, L. K. S.; Recio, M. A. L. *J. Inorg. Biochem.* **2002**, *89*, 212–218.
17. Maeda, M.; Takasura, N.; Suga, T.; Uehara, N.; Hoshi, A. *Anti-Cancer Drugs* **1993**, *4*, 167–171.
18. Tratar Pirc, E.; Arcon, I.; Bukovec, P.; Kodre, A. *Carbohydr. Res.* **2000**, *324*, 275–282.
19. Burger, K.; Takacsi, G.; Nagy, L.; Illes, J.; Stefko, B. Eur. Pat. 413 016 B1, 20 February 1990.
20. Nagy, L.; Yamashita, S.; Yamaguchi, T.; Sipos, P.; Wakita, H.; Nomura, M. *J. Inorg. Biochem.* **1998**, *72*, 49–55.
21. Gilli, R.; Kacurakova, M.; Mathlouthi, M.; Navarini, L.; Paoletti, S. *Carbohydr. Res.* **1994**, *263*, 315–326.
22. Deacon, G. B.; Phillips, R. *J. Coord. Chem. Rev.* **1980**, *33*, 227–250.
23. Stern, E. A.; Newville, M.; Ravel, B.; Yacoby, Y.; Haskel, D. *Physica B* **1995**, *117*, 208–209.
24. Rehr, J. J.; Albers, R. C.; Zabinsky, S. I. *Phys. Rev. Lett.* **1992**, *69*, 3397–3400.
25. Orpen, A. G.; Brammer, L.; Allen, F. H.; Kennard, O.; Watson, D. G.; Taylor, R. *J. Chem. Soc., Dalton Trans.* **1989**, S1–S71.
26. Lys, T. *Acta Crystallogr.* **1979**, *B35*, 1699–1701.
27. Gyurcsik, B.; Nagy, L. *Coord. Chem. Rev.* **2000**, *203*, 81–149.
28. Tratar Pirc, E. T.; Bukovec, P., unpublished results.